Arch. Pharm. Res.
DOI 10.1007/s12272-016-0778-9

RESEARCH ARTICLE

Synthesis of furofuran lignans as antidiabetic agents simultaneously achieved by inhibiting α-glucosidase and free radical

Wisuttaya Worawalai[1] · Phonpimon Khongchai[1] · Nantaporn Surachaitanawat[1] · Preecha Phuwapraisirisan[1]

Received: 24 February 2016 / Accepted: 16 June 2016

Abstract Furofuran lignans such as sesamin have been recognized as promising antidiabetic agents as they possess curative as well as preventive effects toward diabetes complications. However, to date the structure–activity relationship has not been investigated due to the lack of a practical synthetic route capable of producing diverse furofuran lignans. Herein, we first introduced a single-step synthesis of these compounds starting from samin (**4**). Reaction of samin with a variety of electron-rich phenolics under acidic conditions afforded a total of 23 diverse furofuran lignans. On examination their inhibitions against α-glucosidase and free radicals, lignans having a free hydroxy group showed considerably enhanced inhibition, compared with their corresponding starter **4** and related lignans sesamin (**1**) and sesamolin (**3**). In addition, the mechanism underlying the α-glucosidase inhibition of a particular active lignan (***epi*-6**) was verified to be mixed manner between competitive and noncompetitive inhibition.

Keywords *Sesamum indicum* · Diabetes · Glucosidase · Antioxidant · Friedel-Crafts · Oxocarbenium

Introduction

Hyperglycemia in diabetes is the most pivotal initiating cause of impairment of various vulnerable tissues such as capillary endothelial cells in the retina and Schwann cells in peripheral nerves (Brownlee 2005). Prolonged tissue impairment thus results in the rapid incidence of diabetes complications such as cardiomyopathy, nephropathy, neuropathy and retinopathy. To relieve the onset of diabetes and prevent its complications, an alternative approach that concomitantly attenuates the release of glucose from oligosaccharides by blocking the α-glucosidase function and scavenging the causative radicals generated during glycolysis was introduced (Maritim et al. 2003).

This approach prompted us to search for potent antidiabetic agents having dual functions from natural sources (Ramadhan and Phuwapraisirisan 2015a, b) and through semisynthesis (Rattanangkool et al. 2013; Worawalai et al. 2015). Noticeably, introducing polyphenol or phenolic moiety to glucose mimic core structure considerably improved α-glucosidase inhibition together with antioxidation.

In the present communication, we are interested in modifying sesamin (**1**, Fig. 1) structure by replacing methylenedioxybenzene moiety (**A**) with a variety of phenolics (ArOH). This idea was inspired by the considerable evidence concerning its antidiabetic activity as well as other beneficial effects that would alleviate diabetic complications (Hong et al. 2013; Baluchnejadmojarad et al. 2013; Guo et al. 2012; Roghani et al. 2011). Other related structures such as (+)-pinoresinol (**2**) also displayed an antidiabetic effect through inhibiting α-glucosidase (Wikul et al. 2012). Therefore, synthesis of furofuran lignans, the sesamin-like structures, varying with different phenolics could lead to the discovery of new antidiabetic agents that have dual beneficial effects that reduced the administrated dose.

Electronic supplementary material The online version of this article (doi:10.1007/s12272-016-0778-9) contains supplementary material, which is available to authorized users.

✉ Preecha Phuwapraisirisan
preecha.p@chula.ac.th

[1] Natural Products Research Unit, Department of Chemistry, Faculty of Science, Chulalongkorn University, Bangkok, Thailand

Published online: 23 June 2016

To date, there have been two distinct methods employed to synthesize furofuran lignans. Total synthesis starting from small phenolics enabled the construction of the desired lignans (Hull and Knight 1997; Brown et al. 2001; Pohmakotr et al. 2006). However, this methodology could not practically target a wide variety of furofuran lignans due to the low overall yield and limit of phenolics applied. Alternatively, a particular furofuran lignans could be facilely synthesized from naturally abundant precursors such as sesamolin (**3**) in a single step under acidic conditions (Huang et al. 2012; Marchand et al. 1997a). The presence of acetal in sesamolin (**3**) makes it more reactive toward nucleophilic substitution. However, to date, application of **3** as a starter in the synthesis of various furofuran lignans has been limited.

To circumvent the restricted application of **3** in semisynthesis, we introduced the idea of employing samin (**4**), instead of **3**, as the starting material. This approach is based on the fact that hemiacetal moiety in **4** is relatively more reactive, than the acetal residue in **3** toward nucleophilic substitution. In addition, the release of H_2O generated upon protonation of hemiacetal could be readily trapped by a molecular sieve, preventing the regeneration of samin (**4**). Therefore, this proposed methodology would generate the desired furofuran lignans, by varying electron-rich phenolics (ArOH) as nucleophiles (Scheme 1), in sufficient amounts that can be further investigated for structure–activity relationship (SAR).

Materials and methods

General

All moisture-sensitive reactions were carried out under a nitrogen atmosphere. All solvents were distilled prior to use. High resolution electrospray ionisation mass spectra (HRESIMS) was recorded with a Bruker microTof spectrometer. ^{1}H and ^{13}C NMR spectra were recorded ($CDCl_3$ as solvent) at 400 and 100 MHz, respectively, on a Varian Mercury$^+$ 400 NMR and a Bruker (Avance) 400 NMR spectrometer using tetramethylsilane (TMS) as an internal standard. Chemical shifts are reported in ppm downfield from TMS. Analytical thin layer chromatography (TLC) was performed on pre-coated Merck silica gel 60 F_{254} plates (0.25 mm thick layer) and visualized by *p*-anisaldehyde reagent. Column chromatography was performed using Merck silica gel 60 (70–230 mesh) and Sephadex LH-20. Sucrose, maltose and rat intestinal acetone powder were purchased from Sigma-Aldrich (St. Louis, MO, USA). Glucose assay kit was purchased from Human Gesellschaft für Biochemica und Diagnostica mbH (Germany). Acarbose was obtained from Bayer (Germany).

Chemistry

Hydrolysis of sesamolin

To a solution of sesamolin (**3**, 0.27 mmol) in a mixture of acetonitrile/H_2O (9:1, 10 mL) was treated with acidic resin Amberlyst-15 (1 mg/0.005 mmol of **3**). After stirring at 70 °C for 8 h, the reaction mixture was evaporated to dryness and purified by flash chromatography (50 %EtOAc-hexane) to give samin **4** (60 mg, 90 %) as a colorless oil.

Samin (**4**); colorless solid; $[\alpha]_D^{25} = +198$ (*c* 0.1, $CHCl_3$); ^{1}H NMR ($CDCl_3$, 400 MHz) δ 6.85 (s, 1H, H-2′), 6.80–6.75 (m, 2H, H-5′ and H-6′), 5.94 (s, 2H, OCH_2O), 5.36 (s, 1H, H-2), 4.35 (d, J = 8.4 Hz, 2H, H-6 and H-8), 4.16 (dd, J = 9.2, 6.0 Hz, 1H, H-4), 3.89 (d, J = 9.2 Hz, 1H, H-4), 3.56 (dd, J = 8.8, 7.2 Hz, 1H, H-8), 3.25 (brs, 1H, –OH), 3.05 (m, 1H, H-1), 2.86 (m, 1H, H-5); ^{13}C NMR ($CDCl_3$, 100 MHz) δ 148.1, 147.4, 134.7, 119.7, 108.3,

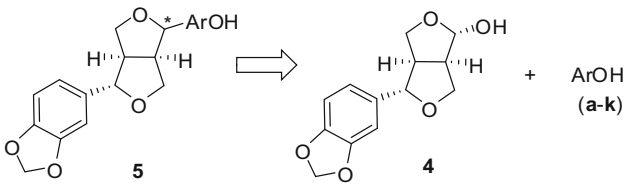

Scheme 1 Synthetic plan for furofuran lignans (**5**) in this work

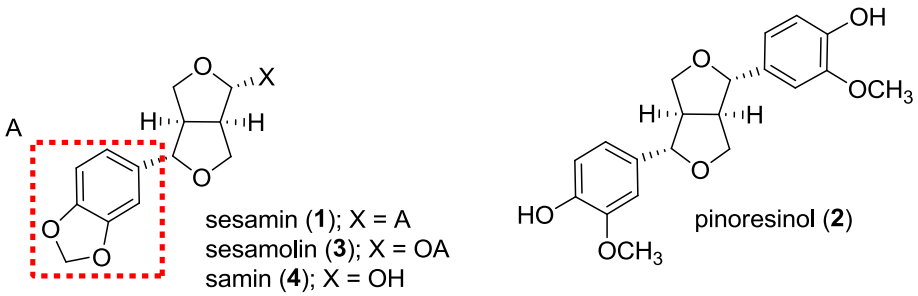

Fig. 1 Structures of selected furofuran lignans

106.7, 102.4, 101.2, 87.0, 71.4, 69.5, 53.7, 52.9. These data coincided well with those in previous report (*J. Agric. Food Chem.*, 2011, **59**, 3214).

General procedure for synthesis of furofuran lignans ***5***

To a solution of samin **4** (1 equiv) in acetonitrile (1.0 mL/0.1 mmol of **4**) was treated with phenolics (1.5–2 equiv), Amberlyst-15 (1 mg/0.005 mmol of **4**) and a 4 Å molecular sieve. After stirring at 70 °C for 8 h, the reaction mixture was evaporated to dryness and purified by flash chromatography.

5a Yield: 30 %, white powder; ^{1}H NMR ($CDCl_3$, 400 MHz) δ 7.89 (brs, 1H, –OH), 6.92 (d, J = 7.6 Hz, 1H, H-6″), 6.83–6.78 (m, 3H, H-2′, H-5′, and H-6′), 6.71 (s, 1H, H-3″), 6.67 (d, J = 7.6 Hz, 1H, H-5″), 5.95 (s, 2H, H-7′), 4.87 (d, J = 4.0 Hz, 1H, H-2), 4.78 (d, J = 4.0 Hz, 1H, H-6), 4.34 (dd, J = 9.2, 7.6 Hz, 1H, H-4), 4.15 (dd, J = 9.2, 6.8 Hz, 1H, H-8), 3.92–3.85 (m, 2H, H-4 and H-8), 3.21 (m, 1H, H-1), 3.14 (m, 1H, H-5), 2.29 (s, 3H, –CH_3); ^{13}C NMR ($CDCl_3$, 100 MHz) δ 155.5, 148.2, 147.4, 139.8, 134.8, 126.8, 120.9, 120.9, 119.5, 117.9, 108.4, 106.7, 101.3, 86.7, 85.6, 72.5, 70.9, 53.6, 53.1, 21.2; HRMS *m/z* 363.1212 $[M + Na]^+$ (calcd for $C_{20}H_{20}NaO_5$, 363.1208).

***epi*-5a** Yield: 15 %, white powder; ^{1}H NMR ($CDCl_3$, 400 MHz) δ 7.85 (brs, 1H, –OH), 6.92 (d, J = 7.6 Hz, 1H, H-6″), 6.86–6.80 (m, 3H, H-2′, H-5′, and H-6′), 6.71 (s, 1H, H-3″), 6.67 (d, J = 7.6 Hz, 1H, H-5″), 5.97 (s, 2H, H-7′), 4.85 (d, J = 5.6 Hz, 1H, H-2), 4.55 (d, J = 8.0 Hz, 1H, H-6), 4.11 (d, J = 9.6 Hz, 1H, H-4), 3.90 (dd, J = 8.4, 7.6 Hz, 1H, H-8), 3.82 (dd, J = 9.6, 6.0 Hz, 1H, H-4), 3.38–3.28 (m, 2H, H-1 and H-8), 3.04 (m, 1H, H-5), 2.29 (s, 3H, –CH_3); ^{13}C NMR ($CDCl_3$, 100 MHz) δ 155.5, 147.9, 146.9, 139.8, 132.0, 126.9, 121.2, 120.8, 118.8, 118.0, 108.4, 106.5, 101.2, 88.6, 82.0, 70.7, 70.2, 53.4, 49.9, 21.3; HRMS *m/z* 363.1213 $[M + Na]^+$ (calcd for $C_{20}H_{20}NaO_5$, 363.1208).

5b Yield: 55 %, colorless oil; ^{1}H NMR ($CDCl_3$, 400 MHz) δ 7.25 (dd, J = 8.0, 2.8 Hz, 1H), 6.84 (s, 1H), 6.81–6.74 (m, 2H), 6.45 (d, J = 7.2 Hz, 1H), 6.44 (d, J = 2.4 Hz, 1H), 5.92 (s, 2H), 5.03 (d, J = 4.8 Hz, 1H), 4.64 (d, J = 5.6 Hz, 1H), 4.30 (dd, J = 9.2, 7.6 Hz, 1H), 4.19 (dd, J = 8.8, 6.4 Hz, 1H), 3.98 (dd, J = 9.2, 5.2 Hz, 1H), 3.90 (dd, J = 9.2, 4.0 Hz, 1H), 3.80 (s, 3H, –OCH_3), 3.79 (s, 3H, –OCH_3), 3.01 (m, 1H), 2.91 (m, 1H); ^{13}C NMR ($CDCl_3$, 100 MHz) δ 160.2, 157.4, 147.9, 147.1, 135.4, 126.1, 122.8, 119.5, 108.1, 106.6, 103.8, 101.0, 98.6, 85.5, 82.0, 73.3, 71.2, 55.4, 55.3, 54.7, 53.7; HRMS *m/z* 393.1310 $[M + Na]^+$ (calcd for $C_{21}H_{22}NaO_6$, 393.1314).

***epi*-5b** Yield: 45 %, colorless oil; ^{1}H NMR ($CDCl_3$, 400 MHz) δ 7.44 (d, J = 8.4 Hz, 1H), 6.87 (s, 1H), 6.81–6.76 (m, 2H), 6.50 (dd, J = 8.4, 2.4 Hz, 1H), 6.44 (s, 1H), 5.94 (s, 2H), 4.91 (d, J = 6.0 Hz, 1H), 4.36 (d, J = 8.0 Hz, 1H), 4.09 (d, J = 9.2 Hz, 1H), 3.81 (s, 3H, –OCH_3), 3.80 (s, 3H, –OCH_3), 3.78–3.74 (m, 2H), 3.47 (m, 1H), 3.22 (dd, J = 8.8, 8.8 Hz, 1H), 2.84 (m, 1H); ^{13}C NMR ($CDCl_3$, 100 MHz) δ 160.2, 156.6, 148.1, 147.3, 135.6, 127.3, 127.3, 119.7, 108.3, 106.8, 103.9, 101.1, 98.3, 87.6, 78.6, 70.5, 69.9, 55.5, 55.4, 54.9, 48.7; HRMS *m/z* 393.1310 $[M + Na]^+$ (calcd for $C_{21}H_{22}NaO_6$, 393.1314).

5c Yield: 20 %, white powder; ^{1}H NMR ($CDCl_3$, 400 MHz) δ 6.94–6.76 (m, 3H), 6.38 (s, 2H), 5.95 (s, 2H), 5.47 (d, J = 5.9 Hz, 1H), 4.70 (d, J = 6.2 Hz, 1H), 4.27 (dd, J = 8.5, 6.6 Hz, 1H), 4.16 (dd, J = 8.9, 7.2 Hz, 1H), 3.89–3.81 (m, 2H), 3.80 (s, 6H, –OCH_3 (×2)), 3.55–3.44 (m, 1H), 3.16–3.01 (m, 1H), 2.33 (s, 3H, –CH_3); ^{13}C NMR ($CDCl_3$, 100 MHz) δ 158.9, 148.0, 147.1, 139.9, 136.0, 119.6, 114.1, 108.3, 106.7, 105.4, 101.1, 85.6, 78.3, 73.2, 72.3, 56.4, 55.9, 51.2, 22.2; HRMS *m/z* 407.1469 $[M + Na]^+$ (calcd for $C_{22}H_{24}NaO_6$, 407.1471).

***epi*-5c** Yield: 21 %, white powder; ^{1}H NMR ($CDCl_3$, 400 MHz) δ 6.91–6.72 (m, 3H), 6.33 (brs, 1H), 6.32 (brs, 1H), 5.96 (s, 2H), 5.22 (d, J = 8.0 Hz, 1H), 4.81 (d, J = 8.0 Hz, 1H), 4.38 (t, J = 8.0 Hz, 1H), 4.10–3.97 (m, 1H), 3.95–3.85 (m, 1H), 3.79 (s, 7H), 3.39–3.27 (m, 1H), 3.24–3.08 (m, 1H), 2.41 (s, 3H, –CH_3); ^{13}C NMR ($CDCl_3$, 100 MHz) δ 160.0, 159.3, 148.1, 147.1, 139.5, 135.8, 135.4, 125.2, 119.5, 108.3, 108.0, 106.7, 101.2, 97.0, 85.1, 81.5, 72.7, 71.9, 55.8, 55.4, 55.4, 52.1, 21.0; HRMS *m/z* 407.1470 $[M + Na]^+$ (calcd for $C_{22}H_{24}NaO_6$, 407.1471).

***epi*-5c′** Yield: 23 %, white powder; ^{1}H NMR ($CDCl_3$, 400 MHz) δ 6.92–6.76 (m, 3H), 6.33 (brs, 1H), 6.32 (brs, 1H), 5.96 (s, 2H), 5.02 (d, J = 7.7 Hz, 1H), 4.82 (d, J = 5.6 Hz, 1H), 4.07 (d, J = 9.3 Hz, 1H), 3.85–3.70 (m, 8H), 3.37 (m,1H), 3.20 (m, 2H), 2.41 (s, 3H, –CH_3); ^{13}C NMR ($CDCl_3$, 100 MHz) δ 159.9, 159.3, 147.7, 146.7, 146.6, 139.7, 132.7, 118.8, 108.2, 108.1, 106.6, 101.1, 96.8, 82.0, 81.9, 71.7, 69.6, 55.9, 55.4, 51.8, 51.1, 20.9; HRMS *m/z* 407.1469 $[M + Na]^+$ (calcd for $C_{22}H_{24}NaO_6$, 407.1471).

5d Yield: 42 %, yellow oil; ^{1}H NMR ($CDCl_3$, 400 MHz) δ 7.16 (d, J = 8.5 Hz, 1H), 6.90–6.72 (m, 3H), 6.63 (d, J = 8.5 Hz, 1H), 5.95 (s, 2H), 5.06 (d, J = 4.0 Hz, 1H), 4.68 (d, J = 4.0 Hz, 1H), 4.30 (t, J = 8.2 Hz, 1H), 4.26–4.13 (m, 1H), 3.98 (dd, J = 9.0, 4.8 Hz, 1H), 3.90 (dd, J = 9.1, 3.9 Hz, 1H), 3.82 (s, 3H, –OCH_3), 3.75 (s, 3H, –OCH_3), 3.10 (m, 1H), 3.00 (m, 1H), 2.16 (s, 3H); ^{13}C NMR ($CDCl_3$, 100 MHz) δ 158.6, 157.0, 148.1, 147.2, 135.5, 127.0, 123.8, 120.1, 119.6, 108.3, 106.7, 106.0, 101.2, 85.7, 82.3, 73.1, 71.5, 60.9, 55.8, 54.8, 54.1, 9.2; HRMS *m/z* 407.1469 $[M + Na]^+$ (calcd for $C_{22}H_{24}NaO_6$, 407.1471).

***epi*-5d** Yield: 31 %, yellow oil; ^{1}H NMR ($CDCl_3$, 400 MHz) δ 7.36 (d, J = 8.6 Hz, 1H), 6.90–6.74 (m, 3H),

6.66 (d, $J = 8.5$ Hz, 1H), 5.94 (s, 2H), 4.96 (d, $J = 6.2$ Hz, 1H), 4.38 (d, $J = 7.4$ Hz, 1H), 4.10 (d, $J = 9.3$ Hz, 1H), 3.83 (m, 4H), 3.74 (m, 4H), 3.46 (m, 1H), 3.24 (t, $J = 8.6$ Hz, 1H), 2.87 (m, 1H), 2.16 (s, 3H); ^{13}C NMR ($CDCl_3$, 100 MHz) δ 158.3, 155.7, 148.1, 147.3, 135.6, 124.5, 124.2, 123.6, 119.8, 108.3, 106.78, 105.9, 101.2, 87.7, 78.8, 70.6, 69.9, 60.6, 55.8, 55.0, 49.3, 9.3; HRMS *m/z* 407.1470 $[M + Na]^+$ (calcd for $C_{22}H_{24}NaO_6$, 407.1471).

5e Yield: 27 %, yellow oil; ^{1}H NMR ($CDCl_3$, 400 MHz) δ 6.89–6.73 (m, 4H), 6.62 (d, $J = 8.6$ Hz, 1H), 5.94 (s, 2H), 5.05 (d, $J = 4.0$ Hz, 1H), 4.68 (d, $J = 4.0$ Hz, 1H), 4.31 (dd, $J = 9.1$, 7.3 Hz, 1H), 4.22 (dd, $J = 9.1$, 6.6 Hz, 1H), 4.01 (dd, $J = 9.2$, 4.7 Hz, 1H), 3.92 (d, $J = 4.3$ Hz, 4H), 3.89 (d, $J = 7.1$ Hz, 4H), 3.10–3.02 (m, 1H), 3.01–2.93 (m, 1H); ^{13}C NMR ($CDCl_3$, 100 MHz) δ 148.1, 147.4, 144.6, 138.7, 135.4, 128.3, 119.6, 115.9, 108.3, 106.7, 105.9, 101.2, 85.6, 82.4, 73.1, 71.6, 60.6, 56.4, 54.8, 54.2; HRMS *m/z* 409.1260 $[M + Na]^+$ (calcd for $C_{21}H_{22}NaO_7$, 409.1263).

***epi*-5e** Yield: 37 %, yellow oil; ^{1}H NMR ($CDCl_3$, 400 MHz) δ 7.02 (d, $J = 8.5$ Hz, 1H), 6.89–6.73 (m, 3H), 6.65 (d, $J = 8.4$ Hz, 1H), 5.95 (s, 2H), 4.95 (d, $J = 5.9$ Hz, 1H), 4.36 (d, $J = 8.0$ Hz, 1H), 4.09 (d, $J = 9.4$ Hz, 1H), 3.97–3.84 (m, 7H), 3.86–3.74 (m, 2H), 3.51–3.40 (m, 1H), 3.24 (t, $J = 8.6$ Hz, 1H), 2.86 (dd, $J = 15.4$, 7.2 Hz, 1H); ^{13}C NMR ($CDCl_3$, 100 MHz) δ 148.1, 147.3, 147.2, 138.2, 135.5, 129.9, 124.6, 119.7, 116.8, 108.3, 106.8, 105.8, 101.2, 87.7, 78.7, 70.6, 69.9, 60.3, 56.4, 54.9, 49.2; HRMS *m/z* 409.1261 $[M + Na]^+$ (calcd for $C_{21}H_{22}NaO_7$, 409.1263).

5f Yield: 31 %, brown oil; ^{1}H NMR ($CDCl_3$, 400 MHz) δ 7.03 (d, $J = 8.6$ Hz, 1H), 6.90–6.73 (m, 3H), 6.64 (d, $J = 8.6$ Hz, 1H), 5.95 (s, 2H), 5.03 (d, $J = 4.0$ Hz, 1H), 4.67 (d, $J = 4.0$ Hz, 1H), 4.33 (dd, $J = 8.9$, 7.5 Hz, 1H), 4.21 (dd, $J = 9.0$, 6.6 Hz, 1H), 3.99 (dd, $J = 8.0$, 4.0 Hz, 1H), 3.92 (s, 3H, –OCH_3), 3.89 (m, 1H), 3.87 (s, 3H, –OCH_3), 3.85 (s, 3H, –OCH_3), 3.05 (m, 1H), 2.98 (m, 1H). ^{13}C NMR ($CDCl_3$, 100 MHz) δ 153.4, 151.2, 148.1, 147.3, 142.4, 135.4, 128.0, 120.3, 119.6, 108.3, 107.1, 106.7, 101.2, 85.6, 82.4, 73.2, 71.5, 60.9, 60.9, 56.2, 54.8, 54.2; HRMS *m/z* 423.1431 $[M + Na]^+$ (calcd for $C_{22}H_{24}NaO_7$, 423.1420).

***epi*-5f** Yield: 22 %, brown oil; ^{1}H NMR ($CDCl_3$, 400 MHz) δ 7.21 (d, $J = 8.6$ Hz, 1H), 6.87–6.76 (m, 3H, H-2′, H-5′, and H-6′), 6.67 (d, $J = 8.6$ Hz, 1H), 5.94 (s, 2H, H-7′), 4.93 (d, $J = 5.6$ Hz, 1H, H-2), 4.37 (d, $J = 8.0$ Hz, 1H, H-6), 4.09 (d, $J = 9.2$ Hz, 1H, H-4), 3.92 (s, 3H, –OCH_3), 3.86 (s, 6H, –OCH_3 (x2)), 3.83–3.77 (m, 2H), 3.43 (m, 1H), 3.24 (m, 1H), 2.86 (m, 1H); ^{13}C NMR ($CDCl_3$, 100 MHz) δ 153.2, 150.0, 148.1, 147.3, 141.8, 135.5, 124.4, 121.2, 119.7, 108.3, 107.0, 106.8, 101.2, 87.7, 78.6, 70.6, 69.9, 60.9, 60.8, 56.1, 55.0, 49.2; HRMS *m/z* 423.1431 $[M + Na]^+$ (calcd for $C_{22}H_{24}NaO_7$, 423.1420).

5g Yield: 68 %, white powder; ^{1}H NMR ($CDCl_3$, 400 MHz) δ 7.71 (brs, 1H, –OH), 6.84–6.79 (m, 3H), 6.54 (s, 1H), 6.49 (s, 1H), 5.96 (s, 2H), 4.82 (d, $J = 8.0$ Hz, 1H), 4.78 (d, $J = 8.0$ Hz, 1H), 4.36 (dd, $J = 8.8$, 7.2 Hz, 1H), 4.16 (dd, $J = 9.6$, 6.4 Hz, 1H), 3.92–3.86 (m, 2H), 3.84 (s, 3H, –OCH_3), 3.82 (s, 3H, –OCH_3), 3.21–3.14 (m, 2H); ^{13}C NMR ($CDCl_3$, 100 MHz) δ 150.3, 150.1, 148.2, 147.4, 142.6, 134.8, 125.2, 119.5, 111.2, 108.4, 106.7, 102.1, 101.3, 86.7, 85.6, 72.6, 70.8, 57.2, 56.1, 53.6, 53.2; HRMS *m/z* 409.1286 $[M + Na]^+$ (calcd for $C_{21}H_{22}NaO_7$, 409.1263).

***epi*-5g** Yield: 17 %, white powder; ^{1}H NMR ($CDCl_3$, 400 MHz) δ 8.05 (brs, 1H, –OH), 6.87–6.77 (m, 3H), 6.46 (s, 1H), 6.42 (s, 1H), 5.95 (s, 2H), 5.01 (d, $J = 8.0$ Hz, 1H), 4.44 (d, $J = 6.8$ Hz, 1H), 4.19 (d, $J = 9.6$ Hz, 1H), 3.98 (t, $J = 8.8$ Hz, 1H), 3.88 (m, 1H), 3.85 (s, 3H, –OCH_3), 3.80 (s, 3H, –OCH_3), 3.49 (dd, $J = 8.4$, 9.2 Hz, 1H), 3.40 (m, 1H), 2.91 (m, 1H); ^{13}C NMR ($CDCl_3$, 100 MHz) δ 150.1, 149.8, 148.2, 147.5, 142.7, 134.8, 125.2, 119.8, 110.5, 108.4, 106.7, 101.9, 101.2, 87.7, 84.6, 71.9, 70.1, 57.0, 56.0, 53.7, 50.8; HRMS *m/z* 409.1275 $[M + Na]^+$ (calcd for $C_{21}H_{22}NaO_7$, 409.1263).

5h Yield: 50 %, colorless oil; ^{1}H NMR ($CDCl_3$, 400 MHz) δ 6.89 (s, 1H), 6.84 (d, $J = 8.0$ Hz, 1H), 6.78 (d, $J = 8.0$ Hz, 1H), 6.13 (s, 2H), 5.95 (s, 2H), 5.42 (d, $J = 6.0$ Hz, 1H), 4.70 (d, $J = 6.0$ Hz, 1H), 4.25 (dd, $J = 8.8$, 6.8 Hz, 1H), 4.16 (dd, $J = 8.8$, 7.2 Hz, 1H), 3.85–3.82 (m, 2H), 3.81 (s, 3H, –OCH_3), 3.80 (s, 6H, –OCH_3 (×2)), 3.49 (m, 1H), 3.07 (m, 1H); ^{13}C NMR ($CDCl_3$, 100 MHz) δ 161.3, 159.9, 159.9, 148.0, 147.1, 136.0, 119.6, 109.6, 108.3, 106.7, 101.1, 91.2, 91.2, 85.6, 78.3, 73.2, 72.2, 56.3, 56.0, 56.0, 55.5, 51.1; HRMS m/z 423.1417 $[M + Na]^+$ (calcd for $C_{22}H_{24}NaO_7$, 423.1420).

5i Yield: 47 %, white powder; ^{1}H NMR ($CDCl_3$, 400 MHz) δ 8.96 (brs, 1H, –OH), 6.82–6.77 (m, 3H), 6.06 (d, $J = 2.4$ Hz, 1H), 6.01 (d, $J = 2.4$ Hz, 1H), 5.95 (s, 2H), 5.21 (d, $J = 4.8$ Hz, 1H), 4.81 (d, $J = 4.0$ Hz, 1H), 4.47 (dd, $J = 9.2$, 8.4 Hz, 1H), 4.13 (dd, $J = 9.2$, 2.8 Hz, 1H), 4.03 (dd, $J = 9.2$, 6.8 Hz, 1H), 3.79 (m, 1H), 3.76 (s, 6H, –OCH_3 (x2)), 3.19 (m, 1H), 3.01 (m, 1H); ^{13}C NMR ($CDCl_3$, 100 MHz) δ 161.0, 158.0, 157.6, 148.2, 147.3, 134.9, 119.5, 108.3, 106.7, 105.0, 101.2, 94.6, 91.0, 84.2, 84.2, 72.7, 71.0, 55.5, 55.5, 54.8, 53.7; HRMS *m/z* 387.1449 $[M + H]^+$ (calcd for $C_{21}H_{23}O_7$, 387.1444).

***epi*-5i** Yield: 51 %, white powder; ^{1}H NMR ($CDCl_3$, 400 MHz) δ 9.15 (brs, 1H, –OH), 6.87–6.77 (m, 3H), 6.07 (d, $J = 2.0$ Hz, 1H), 6.00 (d, $J = 2.4$ Hz, 1H), 5.95 (s, 2H), 5.17 (d, $J = 8.0$ Hz, 1H), 4.40 (d, $J = 6.8$ Hz, 1H), 4.17 (d, $J = 10.0$ Hz, 1H), 3.91 (dd, $J = 8.0$, 8.0 Hz, 1H), 3.81 (dd, $J = 9.6$, 6.4 Hz, 1H), 3.77 (s, 3H, –OCH_3), 3.76 (s, 3H, –OCH_3), 3.51–3.42 (m, 2H), 2.87 (m, 1H); ^{13}C NMR ($CDCl_3$, 100 MHz) δ 160.9, 158.1, 157.4, 148.2, 147.5, 134.9, 119.8, 108.3, 106.8, 101.7, 101.2, 94.3, 90.8,

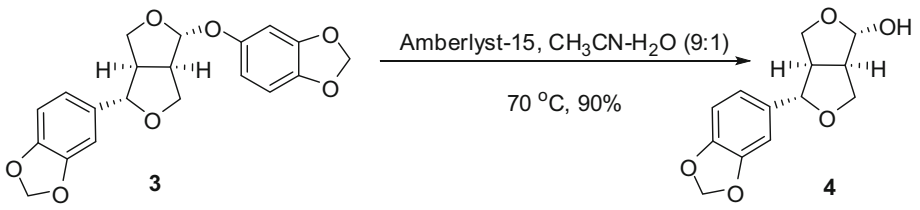

Scheme 2 Synthesis of samin (**4**)

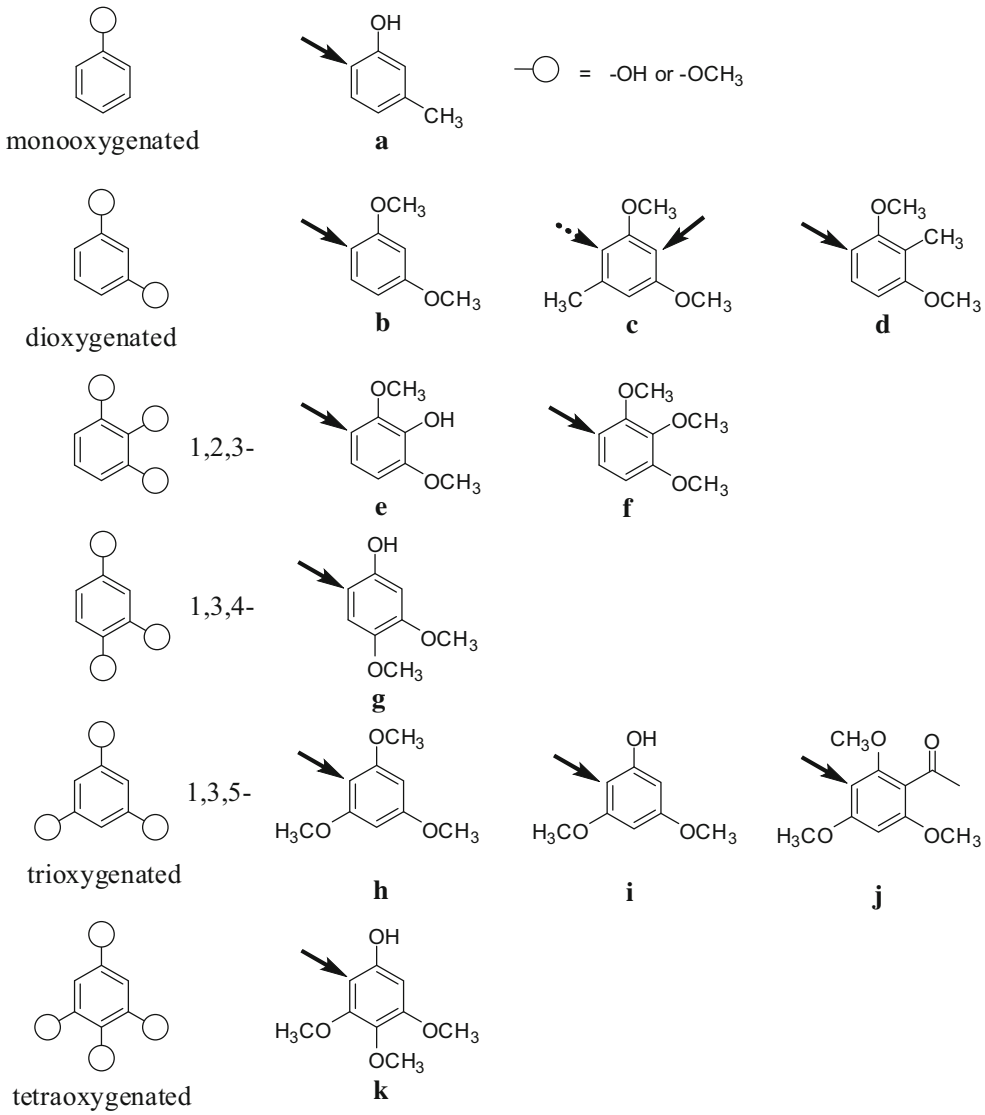

Fig. 2 Phenolics (*a–k*) used in synthesis of furofuran lignans. *Bold arrow* indicates where the bonding between phenolic and furan moiety was formed whereas *dash arrow* suggests another possible regioselective site

87.5, 81.9, 71.4, 70.3, 55.7, 55.4, 53.7, 49.6; HRMS *m/z* 409.1273 $[M + Na]^+$ (calcd for $C_{21}H_{22}NaO_7$, 409.1263).

5j Yield: 15 %, white powder; ^1H NMR ($CDCl_3$, 400 MHz) δ 6.88 (m, 3H), 6.27 (s, 1H), 5.95 (s, 2H), 5.23 (d, $J = 6.0$ Hz, 1H), 4.74 (d, $J = 5.6$ Hz, 1H), 4.31 (dd, $J = 9.2$, 7.2 Hz, 1H), 4.13 (dd, $J = 8.8$, 7.6 Hz, 1H), 3.92–3.90 (m, 2H), 3.85 (s, 3H, $-OCH_3$), 3.83 (s, 3H, $-OCH_3$), 3.77 (s, 3H, $-OCH_3$), 3.44 (m, 1H) 3.12 (m, 1H), 2.49 (s, 3H, $-CH_3$); ^{13}C NMR ($CDCl_3$, 100 MHz) δ 202.0, 160.6, 158.1, 157.8, 148.1, 147.2, 135.7, 119.7, 119.5,

Table 1 Synthesis of furofuran lignans

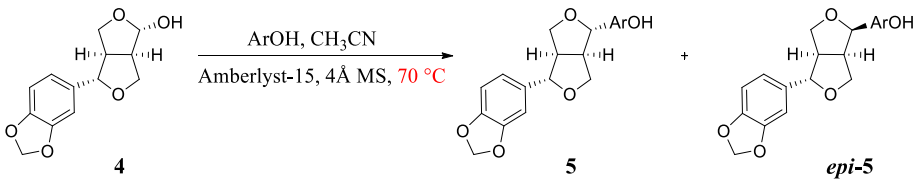

Entry	Isolated product (% yield)	
	5	***epi*-5**
1	**5a** (30 %)	***epi*-5a** (15 %)
2	**5b** (50 %)	***epi*-5b** (45 %)
3	**5c** (19 %)	***epi*-5c** (21 %)
	5c′ (NI)	***epi*-5c′** (24 %)[a]
4	**5d** (31 %)	***epi*-5d** (42 %)
5	**5e** (27 %)	***epi*-5e** (37 %)
6	**5f** (31 %)	***epi*-5f** (22 %)
7	**5g** (68 %)	***epi*-5g** (7 %)
8	**5h** (50 %)	***epi*-5h** (NI)
9	**5i** (51 %)	***epi*-5i** (47 %)
10	**5j** (14 %)	***epi*-5j** (NI)
11	**5k** (30 %)	***epi*-5k** (40 %)

NI not isolated. Due to trace amount, structure characterization and bioactivity evaluation could not be accomplished

[a] The connectivity between furan moiety and 1,3-dimethoxy-5-methylbenzene (**c**) in product ***epi*-5c′** is indicated by a dotted arrow

108.3, 106.7, 101.2, 101.2, 92.0, 85.3, 79.1, 72.8, 72.6, 64.4, 56.0, 56.0, 55.9, 51.5, 29.8; HRMS *m/z* 465.1538 $[M + Na]^+$ (calcd for $C_{24}H_{26}NaO_8$, 465.1525).

5k Yield: 40 %, colorless oil; ^{1}H NMR ($CDCl_3$, 400 MHz) δ 8.58 (brs, 1H, –OH), 6.82–6.77 (m, 3H), 6.22 (s, 1H), 5.95 (s, 2H), 5.12 (d, $J = 8.0$ Hz, 1H), 4.83 (d, $J = 8.0$ Hz, 1H), 4.49 (dd, $J = 8.4$, 8.4 Hz, 1H), 4.13 (dd, $J = 9.6$, 2.8 Hz, 1H), 4.04 (dd, $J = 9.2$, 6.8 Hz, 1H), 3.90 (s, 3H, $–OCH_3$), 3.81 (s, 3H, $–OCH_3$), 3.80 (m, 1H), 3.79 (s, 3H, $–OCH_3$), 3.22 (m, 1H), 3.03 (m, 1H); ^{13}C NMR ($CDCl_3$, 100 MHz) δ 153.9, 152.1, 150.9, 148.2, 147.3, 135.2, 134.7, 119.5, 109.1, 108.4, 106.8, 101.2, 97.0, 84.4, 84.2, 72.9, 70.8, 61.1, 60.9, 56.0, 54.7, 53.7; HRMS *m/z* 439.1366 $[M + Na]^+$ (calcd for $C_{22}H_{24}NaO_8$, 439.1369).

***epi*-5k** Yield: 30 %, colorless oil; ^{1}H NMR ($CDCl_3$, 400 MHz) δ 8.87 (brs, 1H, –OH), 6.87 (s, 1H), 6.83–6.77 (m, 2H), 6.21 (s, 1H), 5.95 (s, 2H), 5.15 (d, $J = 8.0$ Hz, 1H), 4.40 (d, $J = 4.0$ Hz, 1H), 4.18 (d, $J = 10.0$ Hz, 1H), 3.92 (m, 1H), 3.90 (s, 3H, $–OCH_3$), 3.82 (s, 3H, $–OCH_3$), 3.79 (m, 1H), 3.78 (s, 3H, $–OCH_3$), 3.48–3.43 (m, 2H), 2.90 (m, 1H); ^{13}C NMR ($CDCl_3$, 100 MHz) δ 153.8, 152.6, 150.2, 148.2, 147.5, 135.0, 134.8, 119.8, 108.3, 106.7, 105.7, 101.2, 96.8, 87.5, 82.0, 71.4, 70.3, 61.1, 60.9, 55.9, 53.8, 50.2; HRMS *m/z* 439.1366 $[M + Na]^+$ (calcd for $C_{22}H_{24}NaO_8$, 439.1369).

*Synthesis of sesaminol (**6**) and epi-sesaminol (**epi**-6)*

To a solution of sasemolin **3** (82 mg, 0.221 mmol) in acetonitrile (1.5 mL) was treated with acidic resin amberlyst-15 (40 mg). After stirring at 70 °C for 5 h, the reaction mixture was evaporated to dryness and purified by flash chromatography yielding sesaminol (**6**, 66 mg, 80 %) and *epi*-sesaminol (***epi*-6**, 11 mg, 13 %) as a white powder.

Sesaminol (**6**) ^{1}H NMR ($CDCl_3$, 400 MHz) δ 7.76 (brs, 1H, –OH), 6.83–6.78 (m, 3H), 6.51 (s, 1H), 6.45 (s, 1H), 5.96 (s, 2H), 5.89 (s, 2H), 4.77 (d, $J = 4.0$ Hz, 2H), 4.35 (dd, $J = 8.8$, 7.6 Hz, 1H), 4.14 (dd, $J = 9.2$, 6.0 Hz, 1H), 3.89–3.83 (m, 2H), 3.18–3.11 (m, 2H); ^{13}C NMR ($CDCl_3$, 100 MHz) δ 150.9, 148.3, 148.2, 147.4, 141.1, 134.7, 125.2, 119.5, 115.2, 108.4, 106.7, 106.3, 101.3, 99.6, 86.7, 85.5, 72.6, 70.7, 53.5, 53.1; HRMS *m/z* 393.0962 $[M + Na]^+$ (calcd for $C_{20}H_{18}NaO_7$, 393.0950).

epi*-Sesaminol** (epi*-6**) ^{1}H NMR ($CDCl_3$, 400 MHz) δ 8.17 (brs, 1H, –OH), 6.87–6.77 (m, 3H), 6.42 (s, 1H), 6.40 (s, 1H), 5.96 (s, 2H), 5.90 (s, 2H), 4.97 (d, $J = 5.9$ Hz, 1H), 4.41 (d, $J = 7.0$ Hz, 1H), 4.17 (d, $J = 10.0$ Hz, 1H), 4.00 (dd, $J = 9.2$, 8.8 Hz, 1H), 3.84 (dd, $J = 9.6$, 6.4 Hz, 1H), 3.49 (dd, $J = 9.2$, 8.4 Hz, 1H), 3.37 (m, 1H), 2.89 (m, 1H); ^{13}C NMR ($CDCl_3$, 100 MHz) δ 150.8, 148.2, 147.9, 147.5, 141.2, 134.7, 119.8, 112.1, 108.3, 106.7, 105.8,

101.3, 101.2, 99.4, 87.7, 84.5, 71.9, 70.1, 53.6, 50.7; HRMS *m/z* 393.0946 $[M + Na]^+$ (calcd for $C_{20}H_{18}NaO_7$, 393.0950).

α-Glucosidase inhibitory activity

α-Glucosidase inhibitory activity against rat intestinal maltase and sucrase was determined according to our previous report. The crude enzyme solution prepared from rat intestinal acetone powder was used as a source of maltase and sucrase. Rat intestinal acetone powder (1 g) was homogenized in 30 mL of 0.9 % NaCl solution. After centrifugation (12,000*g* × 30 min), the aliquot was subjected to assay. The synthesized compounds (1 mg/mL in DMSO, 10 μL) were added with 30 μL of the 0.1 M phosphate buffer (pH 6.9), 20 μL of the substrate solution (maltose: 10 mM; sucrose: 100 mM) in 0.1 M phosphate buffer, 80 μL of glucose assay kit, and 20 μL of the crude enzyme solution. The reaction mixture was then incubated at 37 °C for 10 min (for maltose) and 40 min (for sucrose). Enzymatic activity was quantified by measuring the absorbance of quinoneimine formed (500 nm) using Bio-Red microplate reader model 3550 UV. The percentage inhibition was calculated by $[(A_0 - A_1)/A_0] \times 100$, where A_0 is the absorbance without the sample, and A_1 is the absorbance with the sample. The IC_{50} value was determined from a plot of percentage inhibition versus sample concentration. Acarbose® was used as the standard control and the experiment was performed in duplicate.

Kinetic study of α-glucosidase inhibition

For kinetic analyses of maltase by the active compound, enzyme and active compounds were incubated with increasing concentrations of maltose (2–20 mM). The type of inhibition was determined by the Lineweaver–Burk plot. For calculation of K_i and K_i' values, slope and intercept from the Lineweaver–Burk plot were replotted vs. [I], which gave the secondary plot.

Antioxidant activities

ABTS (2,2′-azino-bis(3-ethylbenzothiazoline-6-sulfonate) scavenging assay

The radical scavenging activity of synthesized compounds against ABTS·+ was carried out according to a procedure described previously (Hirose et al. 2013). Briefly, ABTS·+ radical cation was produced by mixing 10 mL of 7.4 mM ABTS with 0.5 mL of 2.6 mM potassium persulphate ($K_2S_2O_8$) for 16 h in the dark at room temperature. Before use, the ABTS·+ solution was diluted with ethanol to an absorbance of 0.70 ± 0.02 at 750 nm. The synthesized compounds (20 μL) were mixed with 80 μL of diluted ABTS·+ solution. After 2 h of incubation, the absorbance was read at 750 nm. The percentage inhibition was calculated by $[(A_0 - A_1)/A_0] \times 100$, where A_0 is the absorbance without the sample, and A_1 is the absorbance with the sample. The SC_{50} value was determined from a plot of percentage inhibition versus sample concentration. Butylated hydroxytoluene (BHT) was used as the standard control and the experiment was performed in duplicate.

DPPH (2,2-diphenyl-1-picrylhydrazyl) scavenging assay

Radical scavenging activity was validated using DPPH colorimetric method. Briefly, the synthesized compounds (20 μL) were added to 0.1 mM methanolic solution of DPPH (100 μL). The mixture was kept dark at room temperature in an incubator shaker for 15 min. The absorbance of the resulting solution was measured at 517 nm with a 96-well microplate reader. The percentage inhibition was calculated by $[(A_0 - A_1)/A_0] \times 100$, where A_0 is the absorbance without the sample, and A_1 is the absorbance with the sample. The SC_{50} value was deduced from a plot of percentage inhibition versus sample concentration. BHT was used as the standard control and the experiment was performed in duplicate.

Results and discussion

Synthesis and characterisation

In this experiment, naturally available sesamolin (**3**) was obtained from sesame seed oil using the methodology described elsewhere with minor modification (Reshma et al. 2010). Briefly, sesame seed oil (150 g) dissolved in MeOH (150 mL) was saponified with KOH (25 g) for 2 h. After solvent removal, the resulting mixture was dissolved in water and then extracted with EtOAc. The organic extract mainly containing unsaponifiable lignans was separated on silica gel column using 10 % EtOAc-hexane to obtain sesamin (**1**, 3 g, 2 %) and sesamolin (**3**, 1.5 g, 1 %) (Hemalatha et al. 2004).

Subsequently, we focused our attention on the preparation of samin (**4**) as starting material. Hydrolysis of **3** at 70 °C in MeCN-H_2O (9:1) under acid-catalyzed conditions using Amberlyst-15 (1 mg/0.005 mmol of samin) gave the desired samin (**4**) in 90 % yield (Scheme 2) (Marchand et al. 1997b).

Having the starter **4** in hand, diverse furofuran lignans **5** could be synthesized by nucleophilic substitution (Scheme 1) with a variety of electron-rich phenolics. Under the applied conditions, the reaction is expected to proceed S_N1 fashion via oxocarbenium ion (Huang et al.

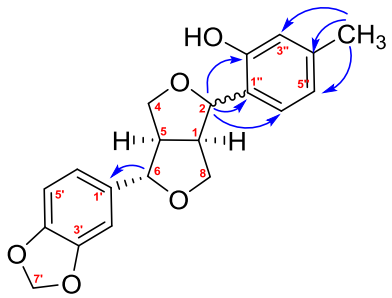

Fig. 3 Selected HMBC correlations of **5a** and ***epi*-5a**

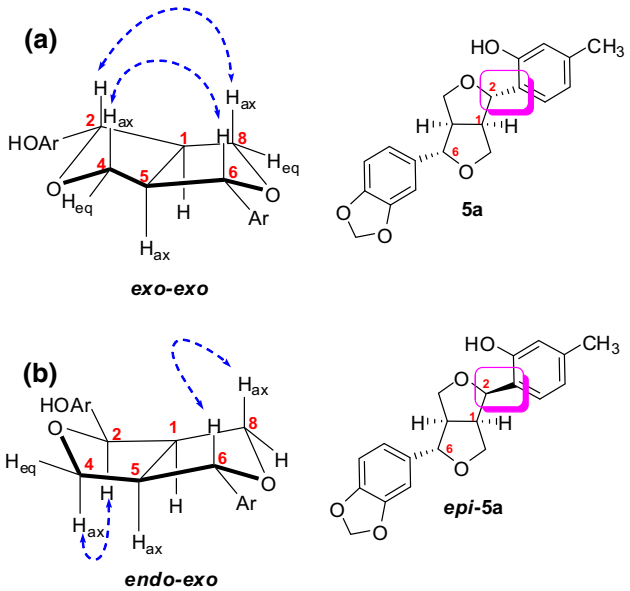

Fig. 4 Diagnostic NOESY correlations of (**a**) **5a** and (**b**) ***epi*-5a**

2012; Marchand et al. 1997a), generated upon protonation with strong acid. In addition, the release of H_2O after the protonation of the hydroxyl group would lead to the regeneration of **4** along with the occurrence of desired products **5**. To prevent unwanted results, removal of H_2O by trapping with a molecular sieve 4Å is required.

With the well-defined synthetic plan in hand, we first applied it in the reaction with monooxygenated benzene. Reaction of **4** and *m*-cresol (**a**, Fig. 2) yielded lignan **5a** (30 %) and its related isomer ***epi*-5a** (15 %) (Table 1). Careful structure elucidation, particularly HMBC analysis, indicated that *m*-cresol was connected to furan moiety through C-2/C-1″ bond formation (Fig. 3).

The relative configuration of **5a** and ***epi*-5a** at C-2 was further determined by NOESY data and coupling constant analysis. The NOESY spectrum of **5a** showed diagnostic correlations of H-2/H-8_{ax} and H-4_{ax}/H-6, suggesting the occupation of two aryls on the *exo–exo* face of the bicyclic core (Fig. 4a). This interpretation was consistent with a boat–boat conformation of sesamin (**1**), which was verified by X-ray analysis (Li et al. 2005). On the other hand, ***epi*-5a** revealed key NOESY correlations of H-2/H-4_{ax} and H-6/H-8_{ax}, which was indicative of *endo-exo*-2,6-diaryl-furofuran (Fig. 4b). These observations correlated well with the chair-boat conformation of *epi*-sesamin or asarinin (Li et al. 2005).

In addition, the difference in the configuration at C-2 of **5a** and ***epi*-5a** could be significantly observed in the ^{1}H NMR pattern and coupling constants of H-2 and neighboring protons. H-2 and H-6 in **5a** each showed doublet signal with comparable coupling constants ($J \approx 4.0$ Hz) whereas those in ***epi*-5a** displayed significantly distinct values; 5.6 Hz for H-2 and 8.0 Hz for H-6. A more strikingly significant observation is the splitting patterns of diastereomeric H_2-4, which appeared as expected as doublet of doublet. However, only H-4_{eq} of ***epi*-5a** showed an exceptional doublet signal caused solely by germinal coupling of H-4_{eq} and H-4_{ax}. This observation would account for a nearly 90° dihedral angle between H-4_{eq} and H-5 that gave rise to $^3J_{4eq,5} \approx 0$ Hz (Günter 1994) (Fig. 5). The above evidence could be useful in readily distinguishing the identity of other synthesized lignans **5** and their epimers.

With the success in applying the above method, we further synthesized other furofuran lignans by varying electron-rich phenolics, namely dioxygenated (**b–d**), trioxygenated (**e–j**) and tetraoxygenated (**k**) benzenes (Fig. 2). All synthesized products (**5b–5k** and their epimers) were securely characterized by ^{1}H, ^{13}C, HRMS as well as 2D NMR where necessary (See also Supplementary Information).

As for regioselectivity, it could be generalized that the product was formed through the carbon–carbon bond between C-2 of furan moiety and phenolic at *ortho*-position to hydroxy or methoxy groups, as indicated by the bold arrows in Fig. 2. This exclusive regioselectivity could be accounted for *ortho*-directing effects of two or more electron-donating groups that reinforce such a preferential electrophilic site for oxocarbenium ion. However, multiple products were also obtained if there was more than one favored site. This observation was demonstrated by the reaction between samin (**4**) and 1,3-dimethoxy-5-methylbenzene (**c**) (Scheme 3). Once the oxocarbenium ion was produced, electrophilic substitution at C-2 of phenolic (pathway A) yielded lignan **5c** and its epimer (***epi*-5c**) while the substitution at C-4 or C-6 (pathway B) afforded lignan **5c′** and its epimer (***epi*-5c′**). Alternatively, these reactions could be described as Friedel–Crafts-like reaction of the phenolic acceptor (Gutmann and Nidetzky 2013).

Alternative, sesaminol (**6**, 80 %) and *epi*-sesaminol (***epi*-6**, 13 %) were also synthesized by refluxing sesamolin (**3**) in Amberlyst-15/acetonitrile (Scheme 4).

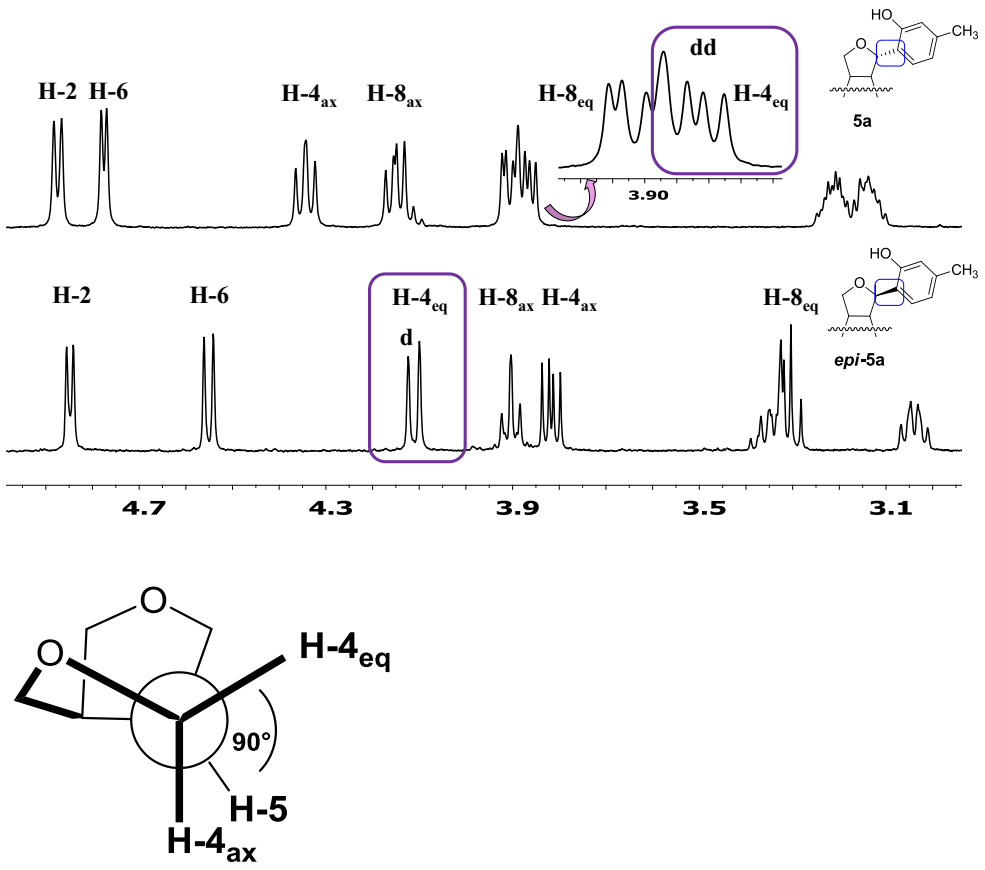

Fig. 5 ^{1}H NMR spectra of **5a** (*top*) and ***epi*-5a** (*bottom*). Note that Newman projection of ***epi*-5a** demonstrates dihedral angle nearly 90° between H-4$_{eq}$ and H-5, thus resulting in doublet (d) signal rather than expected doublet of doublet (dd). For clarity, particular atoms are omitted

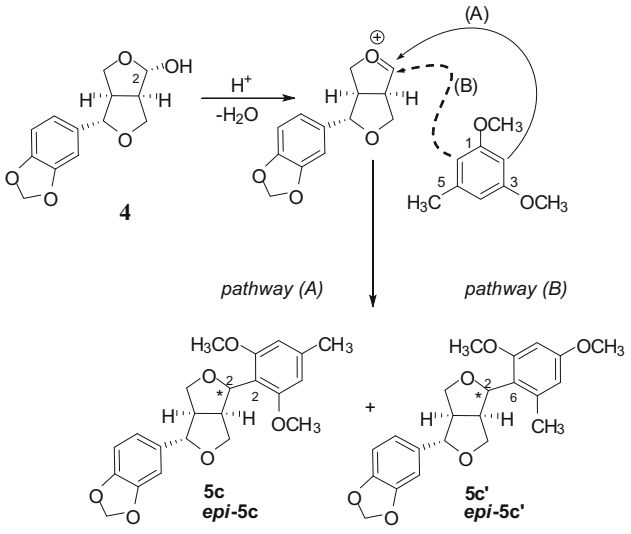

Scheme 3 Mechanistic formation of lignans (**5c**, **5c**′, ***epi*-5c** and ***epi*-5c**′) synthesized from samin (**4**) and 1,3-dimethoxy-5-methylbenzene (**c**)

α-Glucosidase inhibitory and antioxidant activities

All synthesized furofuran lignans were evaluated for α-glucosidase inhibition toward rat intestinal maltase and sucrase as well as antioxidation against DPPH and ABTS radicals (Table 2). Of the products examined, furofuran lignans having free hydroxy group on phenolic moiety, namely **5a**, **5e**, **5g**, **5i**, **5k**, and **6** along with their corresponding epimers, revealed inhibition against both α-glucosidase and free radicals in the range of 1.14–18.9 and 0.15–2.3 mM, respectively. These observations preliminarily suggest that the presence of free hydroxy group plays a critical role in exerting inhibition. For antioxidation, phenolic hydroxyl could donate hydrogen radical (H·) to terminate radical propagation (Yehye et al. 2015), thus preventing the onset of cellular impairment.

Careful inspection on structures of the above active compounds and α-glucosidase inhibition demonstrated intriguing SAR data (Fig. 6). Generally, the epimeric products (designed as ***epi*-**) revealed slightly more potent inhibition (1–3 times) than their corresponding isomers in

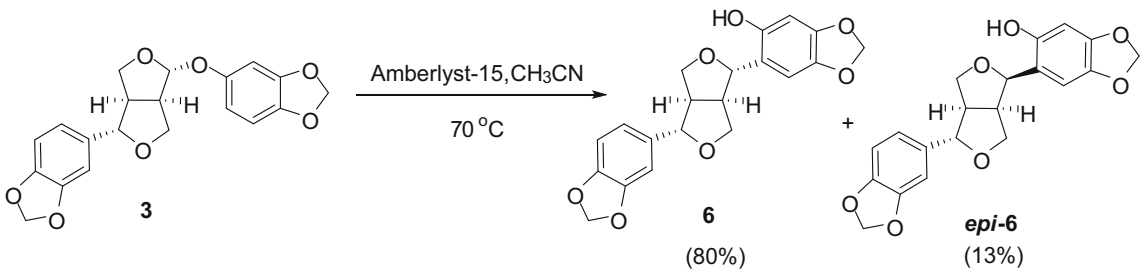

Scheme 4 Synthesis of sesaminol (**6**) and *epi*-sesaminol (***epi*-6**)

Table 2 α-Glucosidase inhibitory effect and radical scavenging activity of furofuran lignans

Compounds	α-Glucosidase inhibitory effect (IC_{50}, mM)		Radical scavenging (SC_{50}, mM)[a]	
	Maltase	Sucrase	DPPH	ABTS
1	NA[b]	NA	NA[b]	NA
3	NA	NA	NA	NA
4	NA	NA	NA	NA
5a	8.23	14.67	NA	0.34
***epi*-5a**	7.01	8.52	NA	0.20
5b	NA	NA	NA	NA
***epi*-5b**	NA	NA	NA	NA
5c	NA	NA	NA	NA
***epi*-5c**	NA	NA	NA	NA
***epi*-5c′**	NA	NA	NA	NA
5d	NA	NA	NA	NA
***epi*-5d**	NA	NA	NA	NA
5e	2.15	3.83	0.34	0.22
***epi*-5e**	1.52	3.13	0.17	0.15
5f	NA	NA	NA	NA
***epi*-5f**	NA	NA	NA	NA
5g	5.59	8.21	0.41	0.34
***epi*-5g**	2.44	3.30	0.22	0.37
5h	NA	NA	NA	NA
5i	4.67	18.89	NA	0.31
***epi*-5i**	2.98	11.1	NA	0.25
5j	NA	NA	NA	NA
5k	3.36	3.59	2.3	0.41
***epi*-5k**	1.31	3.84	1.45	0.40
6	3.42	6.90	0.65	0.39
***epi*-6**	1.14	4.01	0.42	0.35
Acarbose®	0.0015	0.0023	NA	NA
BHT	NA	NA	1.56	0.14

[a] SC_{50}; 50 % radical scavenging concentration

[b] Not active; %inhibition less than 30 % at highest concentration examined against α-glucosidase (0.0625 mg/mL) and radical scavenging (1 mg/mL)

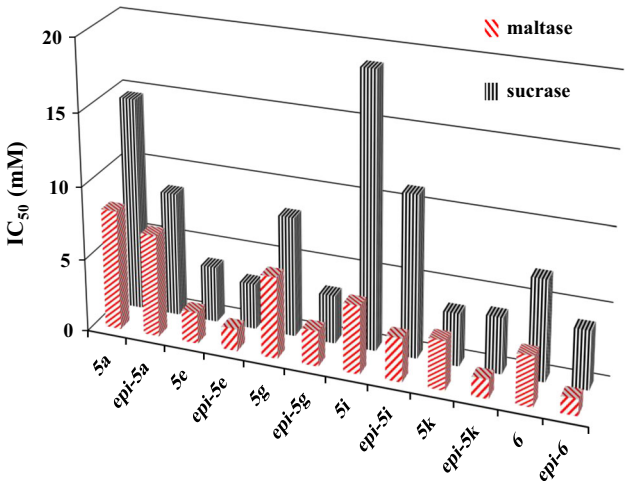

Fig. 6 Intestinal α-glucosidase inhibition of the synthesized lignans containing free hydroxy group at introduced phenolic

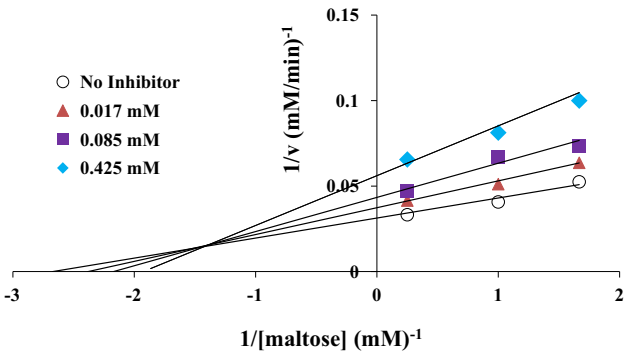

Fig. 7 Lineweaver–Burk plots for inhibitory activity of ***epi*-6** against rat intestinal maltase

all bioassays examined; of which the most significant difference was discovered for **6** and ***epi*-6** (3.42 vs 1.14 mM against maltase). Noticeably, potent inhibition was likely to depend largely on the number of hydroxyls along with other electron donating groups (OMe and Me). These observations were marked by the weaker inhibition of **5a**

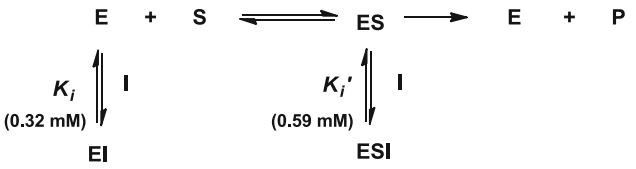

Scheme 5 Putative inhibitory mechanism of ***epi*-6** against rat intestinal maltase. E, S, I and P represent enzyme, substrates (maltose), inhibitors (***epi*-6**) and glucose, respectively

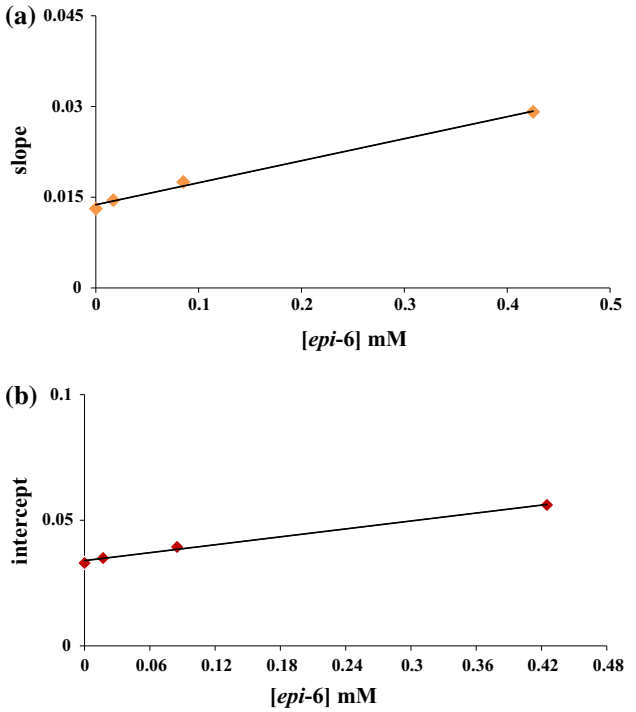

Fig. 8 Secondary replots of (**a**) slope vs. [I] and (**b**) intercept vs. [I] from a primary Lineweaver–Burk plot for the determination of K_i and K'_i, respectively

and ***epi*-5a** (IC_{50} 7.01–14.7 mM), whose phenolics encompassed two electron donating groups (OH and Me). This finding was reversed only for **5i** and ***epi*-5i**, the lignans containing three electron donating groups (OH and 2 × OMe) on the introduced phenolics. To our knowledge, this is the first report on the SAR of lignans.

Kinetic study

To gain insight into the mechanism underlying the inhibitory effect of ***epi*-6**, the representative of synthesized furofuran lignans in this experiment, toward rat intestinal maltase, its kinetic study was performed. Lineweaver–Burk plot of initial velocity versus maltose concentrations in the presence of different concentrations of ***epi*-6** gave a series of straight lines, all of which intersected within the second quadrant (Fig. 7). The analysis displayed an increase in K_m values while V_{max} decrease. This behavior indicated that ***epi*-6** inhibited maltase in a mixed-type manner comprising two different pathways; namely, a competitively forming enzyme-inhibitor (EI) complex and an interrupting enzyme-substrate (ES) intermediate by forming an enzyme-substrate-inhibitor (ESI) complex in a noncompetitive manner (Scheme 5).

We also further investigated the pathway in which ***epi*-6** was preferentially preceded by deducing the dissociation constants of EI (K_i) and ESI (K_i') complexes. Apparently, the secondary plots (Fig. 8) demonstrated K_i and K_i' values of 0.32 and 0.59 mM, respectively, thus indicating that ***epi*-6** was predominantly bound to maltase (EI) rather than the formed ESI complex. The putative inhibitory mechanism is summarized in Scheme 5.

Conclusion

In conclusion, we first synthesized a series of new furofuran lignans by reaction of samin (**4**) and a variety of phenolics in the presence of acidic resin. This approach could be easily conducted in one step, and generated a pair of diastereomeric products, which were useful for investigating the relationship between bioactivity and chemical structure together with stereochemistry. Of the synthesized products, lignans comprising hydroxyl group on the newly introduced phenolic residue demonstrated much more improved inhibition than starter **4** and related lignans **1** and **3** against α-glucosidase and free radicals. The concomitant inhibition of the synthesized compounds would provide benefits both in terms of the curative effect by retarding the enzyme function and the preventive effect by scavenging radicals generated from excess blood glucose. Moreover, the mechanism underlying α-glucosidase inhibition of ***epi*-6**, one of the most potent inhibitor, was proven to inhibit in a mixed-type manner, therefore suggesting that it would be applied as a single diabetic agent or in a combination with antidiabetic drugs such as acarbose. This investigation has provided fundamental clues on the structural motifs required for synthesizing a new series of improved inhibitors and a practical synthetic approach.

Acknowledgments This project was funded by the Thailand Research Fund (RSA5880027) and the Ratchadapisek Sompoch Endowment Fund, Chulalongkorn University (Sci-Super 2014–011). PK and NS are recipients of the Science Achievement Scholarship of Thailand (SAST). Chulalongkorn University Postdoctoral Fellowship to WW is acknowledged. We would also like to express our thanks to Dr. Rico Ramadhan for technical assistance in the kinetic study.

References

Baluchnejadmojarad T, Roghani M, Nadoushan MRJ, Mahdavi MRV, Moghaddam HK, Dehkordi FR, Dariani S, Raoufi S (2013) The sesame lignan sesamin attenuates vascular dysfunction in streptozotocin diabetic rats: involvement of nitric oxide and oxidative stress. Eur J Pharmacol 698:316–321

Brown RCD, Bataille CJR, Hinks JD (2001) Total synthesis of (±)-epimagnolin A. Tetrahedron Lett 42:473–475

Brownlee M (2005) The pathobiology of diabetic complications: a unifying mechanism. Diabetes 54:1615–1625

Günter H (1994) NMR spectroscopy: basic principles, concepts, and applications in chemistry, 2nd edn. John Wiley, New York, pp 115–117

Guo LQ, Yang JR, Kong X (2012) Protective effect of sesamin on endothelial function of type-2 diabetic rats. Chin Pharmacol Bull 28:392–396

Gutmann A, Nidetzky B (2013) Enzymatic *C*-glycosylation: insights from the study of a complementary pair of plant *O*- and *C*-glucosyltransferases. Pure Appl Chem 85:1865–1877

Hemalatha S, Ghafoorunissa (2004) Lignans and tocopherols in Indian sesame cultivars. J Am Oil Chem Soc 81:467–470

Hirose Y, Ohta E, Kawai Y, Ohta S (2013) Dorsamin-A's, glycerolipids carrying a dehydrophenylalanine ester moiety from the seed-eating larvae of the bruchid beetle *Bruchidius dorsalis*. J Nat Prod 76:554–558

Hong L, Yi W, Liangliang C, Juncheng H, Qin W, Xiaoxiang Z (2013) Hypoglycaemic and hypolipidaemic activities of sesamin from sesame meal and its ability to ameliorate insulin resistance in KK-Ay mice. J Sci Food Agric 93:1833–1838

Huang J, Song G, Zhang L, Sun Q, Lu X (2012) A novel conversion of sesamolin to sesaminol by acidic cation exchange resin. Eur J Lipid Sci Technol 114:842–848

Hull HM, Knight DW (1997) Diastereospecific approach to (±)-samin and 2,6-diaryl-3,7dioxabicyclo[3.3.0]octane (furofuran) lignans using the Ireland–Claisen rearrangement of unsaturated oxamacrolides. J Chem Soc Perkin Trans 1(6):857–863

Li CY, Chow TJ, Wu TS (2005) The epimerization of sesamin and asarinin. J Nat Prod 68:1622–1624

Marchand PA, Kato MJ, Lewis NG (1997a) (+)-Episesaminone, a *Sesamum indicum* furofuran lignan.isolation and hemisynthesis. J Nat Prod 60:1189–1192

Marchand PA, Zajicek J, Lewis NG (1997b) Oxygen insertion in *Sesamum indicum* furofuran lignans. diastereoselective syntheses of enzyme substrate analogues. Can J Chem 75:840–849

Maritim AC, Sanders RA, Watkins JB III (2003) Diabetes, oxidative stress, and antioxidants: a review. J Biochem Mol Toxicol 17:24–38

Pohmakotr M, Pinsa A, Mophuang T, Tuchinda P, Prabpai S, Kongsaeree P, Reutrakul V (2006) General strategy for stereoselective synthesis of 1-substituted exo, endo-2,6-diaryl-3,7-dioxabicyclo[3.3.0]octanes: total synthesis of (±)-gmelinol. J Org Chem 71:386–389

Ramadhan R, Phuwapraisirisan P (2015a) Arylalkanones from *Horsfieldia macrobotrys* are effective antidiabetic agents achieved by α-glucosidase inhibition and radical scavenging. Nat Prod Commun 10:325–328

Ramadhan R, Phuwapraisirisan P (2015b) New arylalkanones from *Horsfieldia macrobotrys*, effective antidiabetic agents concomitantly inhibiting α-glucosidase and free radicals. Bioorg Med Chem Lett 25:4529–4533

Rattanangkool E, Kittikhunnatham P, Damsud T, Wacharasindhu S, Phuwapraisirisan P (2013) Quercitylcinnamates, a new series of antidiabetic bioconjugates possessing α-glucosidase inhibition and antioxidant. Eur J Med Chem 66:296–304

Reshma MV, Balachandran C, Arumughan C, Sunderasan A, Sukumaran D, Thomas S, Saritha SS (2010) Extraction, separation and characterisation of sesame oil lignan for nutraceutical applications. Food Chem 120:1041–1046

Roghani M, Baluchnejadmojarad T, Dehkordi FR (2011) The sesame lignan sesamin attenuates vascular permeability in rats with streptozotocin-induced diabetes: involvement of oxidative stress. Int J Endocrinol Metab 9:248–252

Wikul A, Damsud T, Kataoka K, Phuwapraisirisan P (2012) (+)-Pinoresinol is a putative hypoglycemic agent in defatted sesame (*Sesamum indicum*) seeds though inhibiting α-glucosidase. Bioorg Med Chem Lett 22:5215–5217

Worawalai W, Wacharasindhu S, Phuwapraisirisan P (2015) *N*-arylmethylaminoquercitols, a new series of effective antidiabetic agents having α-glucosidase inhibition and antioxidant activity. Bioorg Med Chem Lett 25:2570–2573

Yehye WA, Rahman NA, Ariffin A, Hamid SBA, Alhadi AA, Kadir FA, Yaeghoobi M (2015) Understanding the chemistry behind the antioxidant activities of butylated hydroxytoluene (BHT): a review. Eur J Med Chem 101:295–312